A Fresh Look at the Freshing of the Irminger Current around Cape Farewell, Greenland

Nathan Paldor[1], Ofer Shamir[1], Andreas Münchow[2], A. D. Kirwan, Jr.[2]

[1]Fredy and Nadine Herrmann Institute of Earth Sciences, Hebrew University of Jerusalem, Jerusalem, Israel
[2]School of Marine Science and Policy, University of Delaware, Newark DE, USA

Key Points:

- T-S diagrams clearly show that the freshening is caused by isopycnal mixing in the eastern branch and diapycnal mixing in the western branch
- The Freshening Length paradigm shows that the Irminger Current freshens linearly with downstream distance both east and west of Greenland
- The values of the Freshening Lengths show that the rate of freshening on the eastern branch is 5 times greater than on the western branch

Corresponding author: Nathan Paldor, nathan.paldor@mail.huji.ac.il

Abstract

We estimate the fraction of the Irminger Current that passes from east of Greenland to the Labrador Sea west of Greenland. By employing the new paradigm of Freshening Length we show that only about 20% of the transport east of Greenland navigates its southern tip to enter the Labrador Sea in the west. The other 80% disperses into the ambient ocean. This independent quantitative estimate provides a climatological complement to several recent field campaigns that studied the connection between oceans east and west of Greenland. The Freshening Length approach differs from prior studies, by focusing on the freshening of surface salinity maxima. Surprisingly, these maxima vary nearly linearly with distance along the current's axis and a least-squares fit explains over 90% of the variance. Furthermore, we find that the Irminger Current to the east of Greenland is characterized by isopycnal mixing, while to the west it is characterized by diapycnal mixing.

Plain Language Summary

The subpolar North Atlantic Ocean plays a critical role in global climate change, as it determines how heat and fresh water are distributed across the globe. Boundary current systems around southern Greenland are an important component of this complex process. We examine how ocean temperature, salinity, and currents vary from east to west of Greenland. A new method enables us to determine how much water moves from east to and west of Greenland. We find remarkable robustness in estimates of currents both east and west of the coast of Cape Farewell, Greenland. Ocean freshening of the eastern branch is caused by horizontal motions, whereas in the western branch vertical processes dominate.

1 Introduction

Winds and ocean currents in the subpolar North Atlantic Ocean transform warm and salty surface waters into colder and fresher deep waters via intense air-sea interactions (Marshall & Schott, 1999; Bryden et al., 2020). The deeper waters move southward as the lower limb of the meridional overturning circulation (Cunningham et al., 2007) that extends throughout the world's oceans. A critical region connecting the upper and lower limbs of this Atlantic Meridional Overturning Circulation (AMOC) is just offshore of Greenland. Adjacent to Greenland we find strong boundary current systems (Pickart et al., 2003), vertical convection (de Jong et al., 2012), and deep overflows (Jochumsen et al., 2015) as dynamical ingredients in the exchange of heat and mass between polar and global oceans. Winds and ocean currents around Greenland thus impact regional and global climate at time scales that range from regular weather to glacial cycles (Rahmstorf, 1995, 2002).

Krauss (1986) used drifter and hydrographic observations to quantify the AMOC. He estimated that about 7 Sv of northward flowing warm and salty surface waters are transformed at northern latitudes to cold and deep waters. Initially, it was thought that most of these transformations take place in the Labrador Sea (Pickart et al., 2002), however, more recent observations indicate that most of the deep water formations take place to the east of Greenland both to the north and south of Iceland (Pickart & Spall, 2007; Lozier et al., 2019; de Jong et al., 2012). Lozier et al. (2019) estimate the AMOC from moored ocean velocity, temperature, and salinity observations across the North Atlantic east and west of Greenland. They find an overturning circulation of about 14.9 +/- 0.9 Sv across the subpolar North Atlantic. Almost 90% of this volume flux originates from the Irminger Sea to the east of Greenland (Lozier et al., 2019). The Irminger Sea and upstream oceans to the north thus emerge as the most critical regions in the AMOC.

Thus, it seems that the flow around Cape Farewell at the southern tip of Greenland is a critical component of the complex circulation patterns making up the AMOC.

This is illustrated in Figure 1, adapted from Drinkwater et al. (2020) and Little et al. (2019), which shows two sketches of the circulation of the subpolar North Atlantic. Note the delicate spatial arrangement of the warm and salty Irminger Current adjacent to a cold and fresh East Greenland Current that together form a southward flowing western boundary current (Våge et al., 2011). The East Greenland Current advects polar waters from the Arctic Ocean along the continental slope region to Denmark Strait (Håvik et al., 2017) and beyond (Pickart et al., 2005). Furthermore, a buoyancy-driven coastal current forms from local coastal freshwater discharges as described by Bacon et al. (2002) and Sutherland and Pickart (2008). These southward currents all converge as they approach Cape Farewell. Also noteworthy are the southward currents off East Greenland, which appear to continue northward off West Greenland in Figure 1b only. This western branch of the Irminger Current becomes the West Greenland Current and contains an unknown fraction of Irminger Current waters (Myers et al., 2009). Most of these waters turn cyclonically near 65 N latitude, however, a fraction extends northward into Baffin Bay as a prominent Atlantic temperature maximum that can be traced beyond 78 N latitude (Münchow, 2016; Rignot et al., 2021).

The large number of observational studies conducted in the Irminger and Labrador Seas off southern Greenland inform on the kinematics and dynamics of subpolar boundary currents, deep convection, and climate impacts, e.g., Pickart et al. (2003), Holliday et al. (2007), Myers et al. (2007), Myers et al. (2009), and Le Bras et al. (2020). These studies also describe the seasonal and interannual variability of water properties and transports from moorings and hydrographic expeditions, but such process studies are often limited by their coarse spatial coverage and are not always synoptic.

In contrast, in the present study we analyze 37 years of water properties that are estimated with a data assimilating global model and thus are dynamically consistent with velocity fields. From this data base we quantify the fraction of the Irminger Current to the east of Greenland that successfully negotiates the sharp turn at Cape Farewell and thus contributes to the West Greenland and Baffin Island Currents (Münchow et al., 2015) and eventually the Labrador Current. As was concluded by (Pickart et al., 2003) some of the deep Labrador Sea Water must originate in the Irminger Sea. West Greenland and Irminger Currents are the main conduits for the transport of this water. While much of the Irminger Sea water detaches from the boundaries as it flows into the Labrador Sea near Cape Farewell, we emphasize that an unknown fraction of the Irminger Current continues to flow northward along West Greenland.

To quantify the fraction of the Irminger Current that flows into into Labrador Sea and remains at its surface we appeal to the new paradigm of Evaporation Length developed by Berman et al. (2019). In that study the authors employed the relative changes in the salinity (due to the net evaporation that a column of water undergoes along a trajectory) to calculate a new parameter with the dimension of length termed the Evaporation Length. This method was successively applied to salinity and geochemical data from the Red and Mediterranean Seas, the Indian Ocean, and the Gulf Stream (Berman et al., 2019). Here we adapt that approach to the surface salinity and temperature data for the Irminger Current east and west of Greenland from a data assimilation and ocean reanalysis (Carton et al., 2018). The Evaporation Length estimates the (hypothetical) distance that the column has to travel in order to evaporate all its water. As was shown in Berman et al. (2019) the Evaporation Length reliably quantifies the volume transport of the current per unit length of the cross-stream direction. In the present study we extend this paradigm to the case where the salinity of the water in the column decreases along the trajectory and in this case the new length parameter is termed the Freshening Length. In the scenario considered here the Freshening Length estimates the (hypothetical) distance that the column has to travel in order for its water to become fresh (i.e. zero salinity). The subsequent quantification of the volume transport (per unit length of the cross-stream direction) of the current in the freshening scenario is identical to that

in the evaporation scenario. The paradigm is particularly suitable for use in connection with changes in routinely observed variables (salinity in our case) that are stored in all climatological data archives since it is measured in all observations and reported in all model calculations.

The schema we use is based on long-term observations. It differs from previous studies in that the analysis follows the mean flow and is not limited to brief snapshots in time and not constrained to a specific geographical region. Furthermore, our new metric is insensitive to interannual variations associated with large decadal freshening of the subpolar North Atlantic as described most recently by Holliday et al. (2020). This climatological data base is appropriate for our analysis of the Evaporation Length, because it encapsulates long term trends in the along flow characteristics of salinity and temperature in this region.

The next section of this report describes the data used in our analysis. This is followed by the results of our analysis. The final section discusses our findings in the context of prior works and poses new questions raised by this research.

2 Data and Methods

We use data from the "Simple Ocean Data Assimilation" or SODA project that Carton et al. (2018) describes in technical detail and the National Center for Atmospheric Research distributes at https://rda.ucar.edu/datasets/ds650.0/. The spatial resolution of the gridded data assimilation product is 0.5 degrees in latitude and longitude while the temporal resolution is 5 days. Time series of salinity and temperature data span the period from January 3, 1980 to December 19, 2017, nearly 37 years. The salinity and temperature values presented here are averages over the entire 37-year record taken at a depth of about 5 m. The geographical region used here is 45° W and 35° W longitude between 55° N and 65° N latitude. It covers the ocean adjacent to the southern part of Greenland.

Our first step in the analysis of the average values includes a search, at each latitude, for the longitudes of maximal salinity values on both sides of the 43.75° W longitude. Following this identification of maximal salinity, we average salinity values over 1 degree longitude to the east and west adjacent to the point of maximal salinity, that is, we form a 5-point zonal average centered on the local salinity maximum. We then form transects to the east and west of Cape Farewell (Nunap Isua in Greenlandic) which is the southern tip of Greenland near 44° W longitude and 60° N latitude. The distance along the transect, x, we calculate as the spherical geodesic distance along the trajectory formed by the points of maximal salinity values. Hence Δx is the geodesic distance between two adjacent salinity maxima. Figure 2 shows the location of the zonal salinity maxima to the east (in blue symbols) and west (in red symbols) between Cape Farewell and 63.75° N.

Figure 1 shows the larger geographical context of our study area near Cape Farewell. We adopt this cartoon of the North-Atlantic circulation from Drinkwater et al. (2020) which provides a synopsis of prior results from field studies conducted over the past two decades. It underscores the complexity of the three-dimensional subpolar circulation (Little et al., 2019) as red and dark blue represent warm and cold surface currents, respectively, while light blue reflect deeper flows that result from deep convection or deep overflow from Denmark Strait and the Faroe Channel that both connect the subpolar Atlantic to the Greenland Sea north of Iceland.

3 Results

Figure 2a shows the 37-year mean surface salinity distribution between the Reykjanes Ridge in the east and Labrador in the west. The Reykjanes Ridge to the south of Iceland is part of the Mid-Atlantic Ridge system where salinities and temperatures generally exceed 35 psu and 8 °C, respectively, at the surface. The climatological mean clearly suggests a cyclonic circulation in the Irminger Sea that distributes warm and salty "Irminger Surface Water" preferentially near the 2000-m isobath which is consistent with modern mooring observations (deJong et al., 2020). Note that much fresher waters occupy the continental shelf and slope regions off Greenland delineated by the 1000-m isobath to the east of 55° W longitude (Figure 2). The "Irminger Surface Water" wraps around Cape Farewell and extends northward into the Labrador Sea albeit at reduced salinities and temperatures that we discuss next for the zonal salinity maxima to the east and west of Cape Farewell.

Different mixing regimes are indicated by Figure 3 that shows temperature-salinity (T-S) of surface waters over contours of water density at atmospheric pressure. The data from the eastern (Irminger Current) branch all fall closely on a density contour of 1027.4 $kg\,m^{-3}$. In contrast, the data from the western (West Greenland Current) branch follow an almost straight line that crosses density contours between 1026.6 and 1027.4 $kg\,m^{-3}$ (Figure 3) for locations shown in Figure 2. A comparison between the T-S properties in the two branches shows that freshening occurs along the eastern branch that is density-compensated by cooling. In contrast, the more substantial freshening along the western branch is not density-compensated by cooling. Hence the waters of the western branch become fresher due to diapycnal mixing. While the T-S diagram clearly indicates that different mixing processes act in the two branches, it provides no quantitative information on the **rate** at which the salty water of the Irminger Current freshens as it entrains fresh along its flow. We next introduce an adaptation of the Evaporation Length paradigm to provide a quantitative estimate of the mixing processes in the two branches.

Berman et al. (2019) showed that the inverse of relative salinity changes due to net evaporation along a transect, $S_0/\frac{\Delta S}{\Delta X}$, (where S_0 is the salinity at the origin of the trajectory and $\frac{\Delta S}{\Delta X}$ is the salinity gradient along the trajectory) yields the value of the Evaporation Length denoted by L. The Evaporation Length paradigm requires a moving water column of depth H whose salinity change is determined by the rate at which fresh water is removed from it while its salt content remains unchanged. The conservation of salt and water in the column then relates q and L to the depth H and speed U of the column. We here extend the original evaporation paradigm to the freshening paradigm where the salinity decreases along the trajectory (i.e. $\Delta S < 0$) since fresh water is added to the column e.g. by the entrainment of fresh water from the surrounding sea. In both cases the salinity change of the water in a column that extends from the surface to a depth $z = -H$ yields a length that estimates either the (hypothetical) distance that the column has to travel for all its water to evaporate (in the evaporation paradigm) or for its water to loose all its salinity and become fresh water (in the freshening paradigm). In both cases the Length, L, relates the speed of the current (i.e. the moving column), U, its depth, H, and q — the rate of either net evaporation (in the evaporation paradigm) or fresh water entrainment (in the freshening paradigm).

The Freshening Length paradigm is applied here to the Irminger Current that bifurcates from the salty North Atlantic Current, flows northward along the western flank of the Reykjanes Ridge, turns cyclonically as does the 2000-m isobath, and flows southward along the slope off South-East Greenland (DeJong et al, 2020). Since it is surrounded by fresher waters on both the Greenland's shelf and the Irminger Sea sides (Figure 2), it is clearly identified by a local salinity maximum.

Note that the two branches shown in figure 4 are continued from the right bottom corner of panel (b) to the upper left corner of panel (a). The least squared best fitting

lines in the two panels of Figure 4 were calculated using the Matlab curve-fitting tool. Figure 4 clearly shows that the Freshening Length, L, on Greenland's east side (10^6 Km, panel b) is five times larger than that on the west side (0.2×10^6 Km, panel a). The correlated variance R^2 of salinity and distance along the transect to the east and west off Greenland are larger than 0.92 and 0.97, respectively. Moreover, the transect along the eastern branch starts at 63.75N and extends to the south-west, while the transect along the westward branch starts at 58.75N and extends to the north-west to the same 63.75N latitude.

Berman et al. (2019) demonstrated that the value of L is related to the volume transport per unit length of the cross-stream direction $F = H \times U$ via:

$$Lq = F. \tag{1}$$

Clearly, the 5-fold higher L of the Irminger Current in the east branch relative to the west branch has direct consequences on the transport of the Current, F, and/or on the rate of fresh water entrainment, q, in the two branches.

4 Discussion

The fate of salty and warm Atlantic water of subtropical origin plays an important role in the AMOC. Here we diagnose the salinity gradient along its path adjacent to southern Greenland. Figure 1 shows two different sketches of the circulation with red pathways that represent the near-surface circulation in both the Irminger Sea to the east and the Labrador Sea to the west of Greenland. In Figure 1a the Irminger Current does not navigate Cape Farewell, but instead blends into the ambient Labrador Sea as the atmosphere removes its heat. In contrast, Figure 1b shows that a fraction of the Irminger Current navigates around Cape Farewell to flow along the slope of West Greenland (Pacini et al., 2020). Another fraction retroflects back into the Irminger Sea to contribute to an anti-cyclonic gyre there. Holliday et al. (2007) estimate that about 5.1 Sv or 80% of Irminger Current retroflects. Our Freshening Length results suggest the same percentage of retroflection at Cape Farewell.

The T-S plot in figure 3 shows that the southernmost stations on the east and west branches of the Current have nearly identical water mass characteristics, even though they are over 75 km apart. This implies continuity of the two branches of the Irminger Current. Moreover, Figure-2 emphasizes different freshening mechanisms of the Irminger Current east and west of Greenland. The eastern branch exhibits typical isopycnal mixing from the northern start to the southern end, a distance of about 700 kilometers. We interpret this isopycnal mixing as horizontal entrainment along a density surface. This conclusion is consistent with those drawn by both Pickart et al. (2003) and Smith (1937). While the former employed modern moorings and cross-sectional hydrography, early American (Smith, 1934) and Scandinavian (reference) studies provided similar descriptions as part of the International Ice Patrol instead of the climatological data used here.

In contrast, the western branch of the Irminger Current is characterized by strong diapycnal exchange that indicates vertical mixing. This, too, is consistent with Pickart et al. (2003) who concluded that the source of the North Atlantic Deep Water originates in the Irminger Sea rather than the Labrador Sea. The distinctive difference of horizontal and vertical mixing to the east and west of Greenland, respectively, resolves the discrepancy in circulations in Figure 1. Our analysis suggests that only about 20% of the eastern branch of the Irminger Current continues northwestward along West Greenland.

Our analysis of the SODA climatological salinity transects along the Irminger current employs the Freshening Length paradigm recently proposed in Berman et al. (2019). Our analysis yields a 5-fold difference in L between the two branches. What does this finding imply? There are two possible scenarios:

In a first scenario, if we assume equal fresh water entrainment rates, q, into the Irminger Current east and west of Greenland, then the equatorward transport of the Irminger Current off East Greenland is 5-times larger than that the poleward transport off West Greenland. Hence we conclude that only 20% of the eastern branch successfully negotiates the sharp turn at Cape Farewell. For a uniform q the 80% decrease in L from 1×10^6 km in the east branch to 0.2×10^5 km in the west branch implies that 80% of the Irminger Current detaches from the coast. We speculate that some of this 80% may cool, sink, and contribute to the NADW as Drinkwater et al. (2020) suggested with the purple cyclone labeled "LS" in Figure 1a. Alternatively, some of these 80% could retroflect and form the southern branch of the Irminger Gyre as depicted in 1b and labeled "IC". Holliday et al. (2007) quantifies such a retroflection from a single snapshot of velocity observations, however, they find 80% navigate the bend of Cape Farewell from east to west while 20% moves offshore and to the east. And finally, we speculate that a fraction the 80% is shed as eddies in the area (Bracco et al., 2008).

In a second scenario, the fresh water entrainment rate, q, is 5 times larger in the western branch compared to the east branch. This counterbalances the difference in L so that the volume transports F in the two branches are similar. This scenario requires that the speed of the current decreases in the west branch, to allow for the higher rate of entrainment, while the depth of the current increases to maintain the same volume transport.

The SODA3 data contains annual and seasonal variations of surface salinity and Freshening Lengths in addition to the 37-year mean discussed above. Repeating the above analyses on annual data, we find root-mean-square variations of the Freshening Length of about 300 km, i.e. less than 1%, (not shown). Variations include physical signals such as the Great Salinity Anomalies in 1981 and 1993 (Belkin, 2004) that propagate through the subpolar North Atlantic Ocean with surface salinities, S(x=0), that are more than 0.4 psu below the SODA3 average both east and west of Greenland. During 1995 and 2016 we find almost uniform salinity along the axis of the Irminger Current east of Greenland (not shown) which implies infinitely large Freshening Length. Our findings are consistent with those of Holliday et al. (2020) who find substantial expansion of the Irminger Gyre in recent years. Nevertheless, the combination of climatological data and Freshening Length paradigm emerges as a robust metric largely insensitive to decadal events like the Great Salinity Anomalies in the subpolar Atlantic Ocean (Belkin, 2004; Holliday et al., 2020).

We stress that our analysis uses 37 years of assimilated modeled hydrographic data and a new paradigm. This Freshening Length paradigm compliments traditional studies that emphasize direct data from moorings and surveys of the Irminger Current to the east and west of Greenland. It would be interesting to examine survey data along the axis of the Irminger Current, as done here, to compare with the climatological analysis presented here. Such hydrographic data from the center of the Irminger Current may resolve the dynamics that lead to the two scenarios presented above. Only direct observations can decide whether the 5-fold drop in the value of L along the east branch corresponds to a drop in the transport F of the current as it negotiates Cape Farewell.

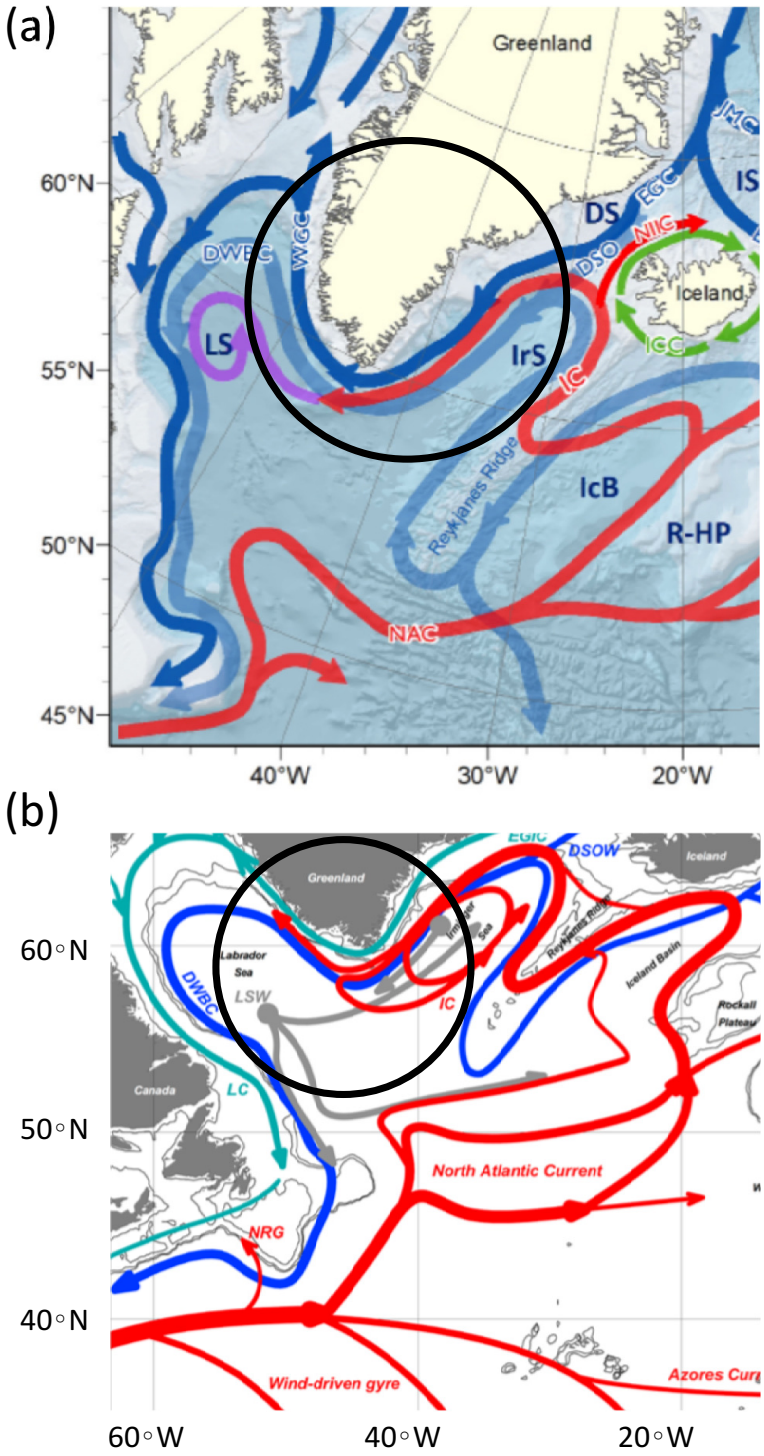

Figure 1. Two sketches of the North-Atlantic circulation between Iceland in the north-east and Newfoundland in the south-west adapted from (a) Drinkwater et al. (2020) and (b) Little et al. (2019). Red currents indicate warm and salty surface waters. Light blue currents in (a) and blue currents in (b) indicate cooler deeper flows. The dark blue lines in (a) and turquoise lines in (b) indicate cold and fresh Arctic surface waters such as the East Greenland and Labrador Currents to the east of Greenland and Labrador, respectively. Grey dots and arrows in (b) indicate deep water formation areas in the Labrador and Irming Seas. Black circles focus on the Irminger Current at the southern tip of Greenland.

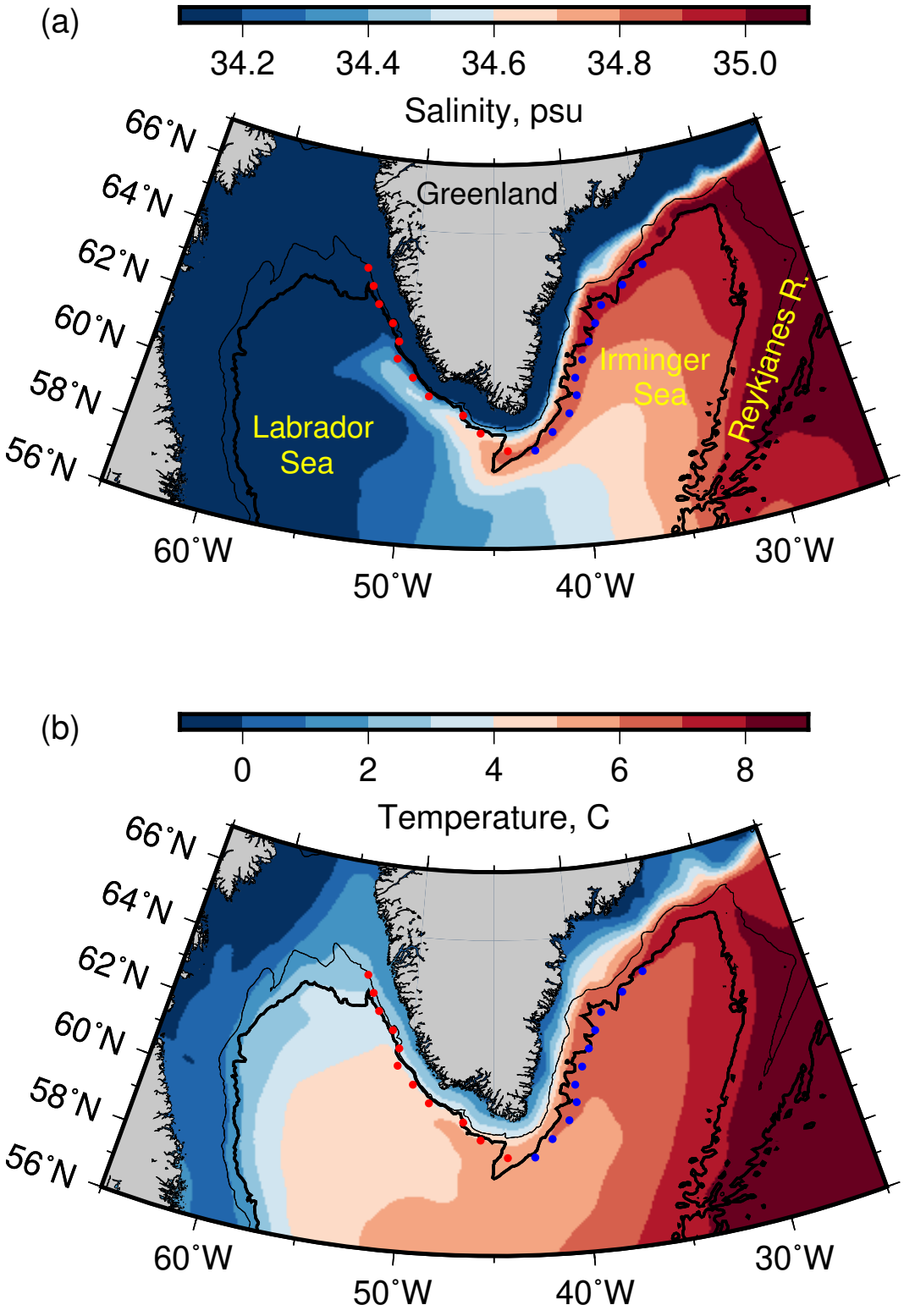

Figure 2. 37-year averages of surface salinity in psu (a) and temperature in °C (b) around southern Greenland. Blue and red filled circles indicate the location of eastern and western salinity maxima, respectively, along constant longitudes. Black contours are 1000 m and 2000 m bottom depths.

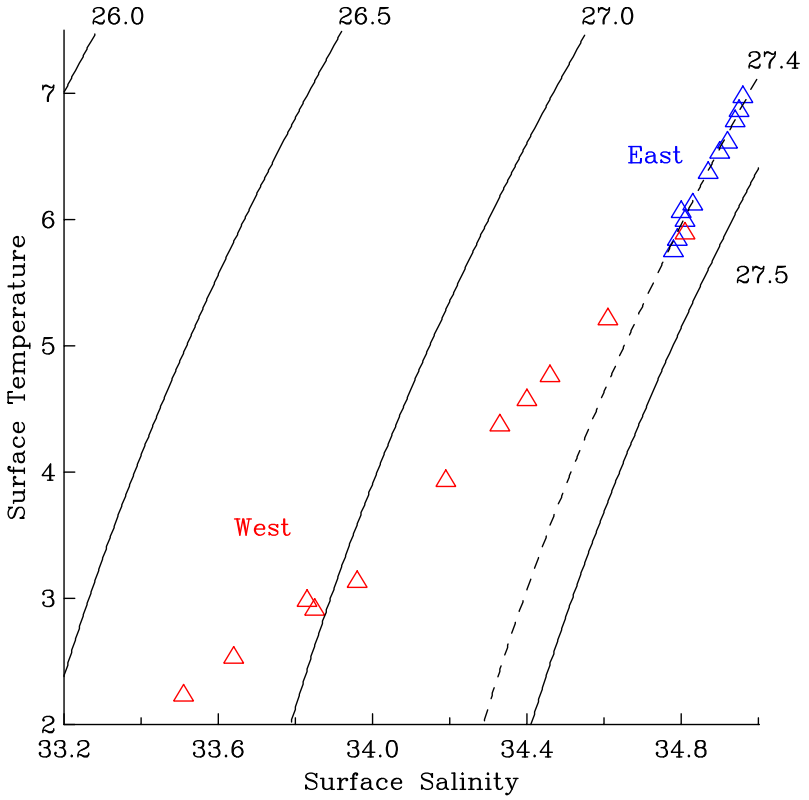

Figure 3. Surface temperature-salinity diagram (triangular symbols) over density contours (solid and dashed thin lines) for the stations shown in Figure 2 and used in Figure 4. Red and blue triangles are from stations along the western and eastern branches, respectively.

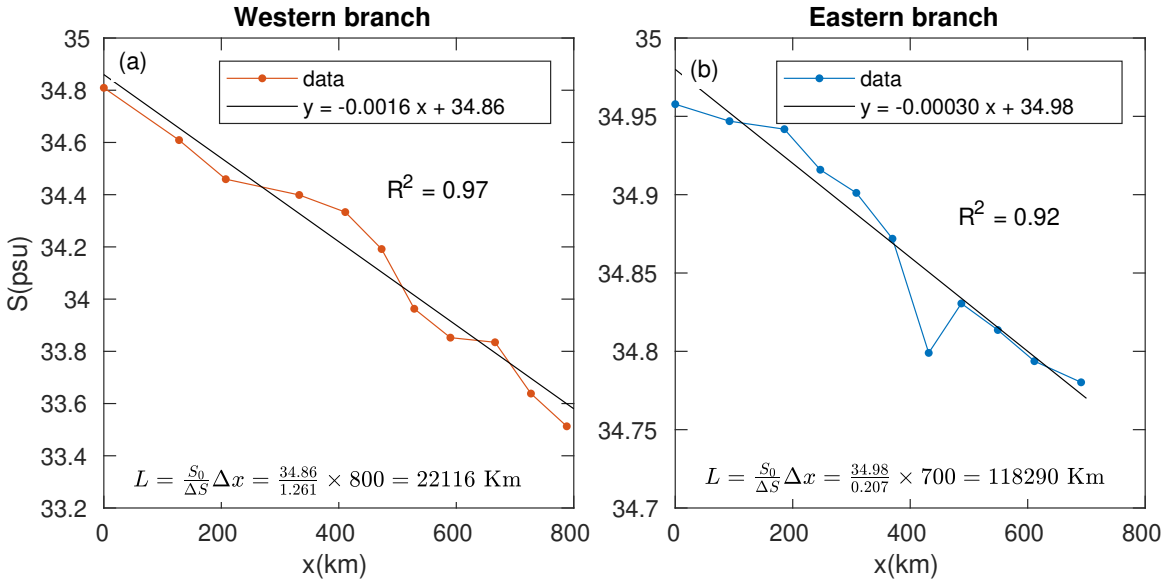

Figure 4. Salinity (psu) along the trajectories highlighted in figure 2. The salinity in each branch is averaged over the 5 grid points containing the maximum and two adjacent grid points on either sides of the maximum. x is the spherical geodesic distance along the trajectory, i.e. Δx is the geodesic distance between two adjacent maxima. The linear fits were calculated using Matlab curve-fitting tool to find the least square linear fit.

Acknowledgments

The authors are grateful for not having any financial support for this research. The data used in this study are available from SODA website: https://rda.ucar.edu/datasets/ds650.0/.

References

Bacon, S., Reverdin, G., Rigor, I. G., & Snaith, H. M. (2002). A freshwater jet on the East Greenland shelf. *J. Geophys. Res.*, *107*(C7), 3068.

Belkin, I. M. (2004). Propagation of the "Great Salinity Anomaly" of the 1990s around the northern North Atlantic. *Geophys. Res. Let.*, *31*(8), L08306.

Berman, H., Paldor, N., Churchill, J., & Lazar, B. (2019). Constraining evaporation rates based on large-scale sea surface transects of salinity or isotopic compositions. *J. Geophys. Res. Oceans*, *124*(2), 1322–1330.

Bracco, A., Pedlosky, J., & Pickart, R. S. (2008). Eddy formation near the west coast of Greenland. *J. Phys. Oceanogr.*, *38*(9), 1992–2002.

Bryden, H. L., Johns, W. E., King, B. A., McCarthy, G., McDonagh, E. L., Moat, B. I., & Smeed, D. A. (2020). Reduction in ocean heat transport at 26n since 2008 cools the eastern subpolar gyre of the North Atlantic Ocean. *Journal of Climate*, *33*(5), 1677–1689.

Carton, J. A., Chepurin, G. A., & Chen, L. (2018). Soda3: A new ocean climate reanalysis. *Journal of Climate*, *31*(17), 6967–6983.

Cunningham, S. A., Kanzow, T., Rayner, D., Baringer, M. O., Johns, W. E., Marotzke, J., ... Bryden, H. L. (2007). Temporal variability of the Atlantic Meridional Overturning Circulation at 26.5N. *Science*, *317*(5840), 935–.

de Jong, M. F., van Aken, H. M., Vage, K., & Pickart, R. S. (2012). Convective mixing in the central Irminger Sea: 2002-2010. *Deep Sea Research Part I: Oceanographic Research Papers*, *63*, 36–51.

Drinkwater, K. F., Sundby, S., & Wiebe, P. H. (2020). Exploring the hydrography of the boreal/arctic domains of North Atlantic seas: Results from the 2013 BASIN survey. *Deep Sea Research Part II: Topical Studies in Oceanography*, *180*, 104880–.

Holliday, N. P., Bersch, M., Berx, B., Chafik, L., Cunningham, S., Florindo-Lòpez, C., ... Yashayaev, I. (2020). Ocean circulation causes the largest freshening event for 120 years in eastern subpolar North Atlantic. *Nature Communications*, *11*(1), 585–.

Holliday, N. P., Meyer, A., Bacon, S., Alderson, S. G., & de Cuevas, B. (2007). Retroflection of part of the East Greenland Current at Cape Farewell. *Geophys. Res. Lett.*, *34*(7), –.

Håvik, L., Pickart, R., Våge, K., Torres, D., Thurnherr, A., Beszczynska-Möller, W., Walczowski, & von Appen, W.-J. (2017). Evolution of the East Greenland Current from Fram Strait to Denmark Strait: Synoptic measurements from summer 2012. *J. Geophys. Res.*, *122*, 1974-1994. doi: 10.1002/2016JC012228

Jochumsen, K., Köllner, M., Quadfasel, D., Dye, S., Rudels, B., & Valdimarsson, H. (2015). On the origin and propagation of Denmark Strait overflow water anomalies in the Irminger Basin. *J. Geophys. Res. Oceans*, *120*(3), 1841–1855.

Krauss, W. (1986). The North Atlantic Current. *J. Geophys. Res.*, *91*(C4), 5061–5074.

Le Bras, I. A.-A., Straneo, F., Holte, J., de Jong, M. F., & Holliday, N. P. (2020). Rapid export of waters formed by convection near the Irminger Sea's western boundary. *Geophys. Res. Lett.*, *47*(3), e2019GL085989–.

Little, C. M., Hu, A., Hughes, C. W., McCarthy, G. D., Piecuch, C. G., Ponte, R. M., & Thomas, M. D. (2019). The relationship between U.S. East Coast sea level and the Atlantic Meridional Overturning Circulation: A review. *J. Geophys. Res. Oceans*, *124*(9), 6435–6458.

Lozier, M. S., Li, F., Bacon, S., Bahr, F., Bower, A. S., Cunningham, S. A., ... Zhao, J. (2019). A sea change in our view of overturning in the subpolar North Atlantic. *Science*, *363*(6426), 516–.

Marshall, J., & Schott, F. (1999). Open-ocean convection: Observations, theory, and models. *Rev. Geophys.*, *37*(1), 1–64.

Münchow, A. (2016). Volume and freshwater flux observations from Nares Strait to the west of Greenland at daily time scales from 2003 to 2009. *J. Phys. Oceanogr.*, *46*(1), 141–157. doi: 10.1175/JPO-D-15-0093.1

Münchow, A., Falkner, K., & Melling, H. (2015). Baffin Island and West Greenland Current systems in northern Baffin Bay. *Progress In Oceanography*, *132*, 305-317.

Myers, P. G., Donnelly, C., & Ribergaard, M. H. (2009). Structure and variability of the West Greenland Current in summer derived from 6 repeat standard sections. *Progr. Oceanogr.*, *80*(1-2), 93–112.

Myers, P. G., Kulan, N., & Ribergaard, M. H. (2007). Irminger Water variability in the West Greenland Current. *Geophys. Res. Lett.*, *34*(17), –.

Pacini, A., Pickart, R. S., Bahr, F., Torres, D. J., Ramsey, A. L., Holte, J., ... Femke de Jong, M. (2020). Mean conditions and seasonality of the West Greenland Boundary Current System near Cape Farewell. *Journal of Physical Oceanography*, *50*(10), 2849–2871.

Pickart, R. S., & Spall, M. A. (2007). Impact of Labrador Sea convection on the North Atlantic Meridional Overturning Circulation. *Journal of Physical Oceanography*, *37*(9), 2207–2227.

Pickart, R. S., Straneo, F., & Moore, G. (2003). Is Labrador Sea Water formed in the Irminger basin? *Deep Sea Research Part I: Oceanographic Research Papers*, *50*(1), 23–52.

Pickart, R. S., Torres, D. J., & Clarke, R. A. (2002). Hydrography of the labrador sea during active convection. *Journal of Physical Oceanography*, *32*(2), 428–457.

Pickart, R. S., Torres, D. J., & Fratantoni, P. S. (2005). The East Greenland Spill Jet. *Journal of Physical Oceanography*, *35*(6), 1037–1053.

Rahmstorf, S. (1995). Bifurcations of the Atlantic thermohaline circulation in response to changes in the hydrological cycle. *Nature*, *378*(6553), 145–149.

Rahmstorf, S. (2002). Ocean circulation and climate during the past 120,000 years. *Nature*, *419*(6903), 207–214.

Rignot, E., An, L., Chauche, N., Morlighem, M., Jeong, S., Wood, M., ... Münchow, A. (2021). Retreat of Humboldt Gletscher, North Greenland, driven by undercutting from a warmer ocean. *Geophys Res Lett*, *48*(6), e2020GL091342–.

Sutherland, D. A., & Pickart, R. S. (2008). The East Greenland Coastal Current: Structure, variability, and forcing. *Progr. Oceanogr.*, *78*(1), 58–77.

Våge, K., Pickart, R. S., Sarafanov, A., Knutsen, Ø., Mercier, H., Lherminier, P., ... Bacon, S. (2011). The Irminger Gyre: Circulation, convection, and interannual variability. *Deep Sea Research Part I: Oceanographic Research Papers*, *58*(5), 590–614.